Clinical and Translational Radiation Oncology 36 (2022) 99–105

Contents lists available at ScienceDirect

Clinical and Translational Radiation Oncology

journal homepage: www.sciencedirect.com/journal/clinical-and-translational-radiation-oncology

Original Research Article

Time- and dose-dependent volume decreases in subcortical grey matter structures of glioma patients after radio(chemo)therapy

F. Raschke [a,b], K. Witzmann [a,b], A. Seidlitz [b,c], T. Wesemann [d], C. Jentsch [b,c], I. Platzek [f], J. van den Hoff [g], J. Kotzerke [h], B. Beuthien-Baumann [i], M. Baumann [b,j], J. Linn [d], M. Krause [a,b,c,e,k], E.G.C. Troost [a,b,c,e,k,*]

[a] Institute of Radiooncology - OncoRay, Helmholtz-Zentrum Dresden-Rossendorf, Rossendorf, Germany
[b] OncoRay - National Center for Radiation Research in Oncology, Faculty of Medicine and University Hospital Carl Gustav Carus, Technische Universität Dresden, Helmholtz-Zentrum Dresden – Rossendorf, Dresden, Germany
[c] Department of Radiotherapy and Radiation Oncology, Faculty of Medicine and University Hospital Carl Gustav Carus, Technische Universität Dresden, Dresden, Germany
[d] Institute of Neuroradiology, University Hospital Carl Gustav Carus and Medical Faculty of Technische Universität, Dresden, Germany
[e] German Cancer Consortium (DKTK), Partner Site Dresden, and German Cancer Research Center (DKFZ), Heidelberg, Germany
[f] Faculty of Medicine and University Hospital Carl Gustav Carus, Technische Universität Dresden, Department of Diagnostic and Interventional Radiology, Dresden, Germany
[g] Helmholtz-Zentrum Dresden - Rossendorf, Institute of Radiopharmaceutical Cancer Research, Center for Positron Emission Tomography, Dresden-Rossendorf, Germany
[h] Faculty of Medicine and University Hospital Carl Gustav Carus, Technische Universität Dresden, Department of Nuclear Medicine, Dresden, Germany
[i] Radiology, German Cancer Research Center (DKFZ), Heidelberg, Germany
[j] German Cancer Research Center (DKFZ), Heidelberg, Germany
[k] National Center for Tumor Diseases (NCT), Partner Site Dresden, Germany: German Cancer Research Center (DKFZ), Heidelberg, Germany; Faculty of Medicine and University Hospital Carl Gustav Carus, Technische Universität Dresden, Dresden, Germany, and; Helmholtz Association / Helmholtz-Zentrum Dresden - Rossendorf (HZDR), Dresden, Germany;

ARTICLE INFO

Keywords:
Hippocampus
Amygdala
Radiotherapy
Atrophy
Proton therapy
Caudate

ABSTRACT

Background and purpose: Radiotherapy (RT) is an adjuvant treatment option for glioma patients. Side effects include tissue atrophy, which might be a contributing factor to neurocognitive decline after treatment. The goal of this study was to determine potential atrophy of the hippocampus, amygdala, thalamus, putamen, pallidum and caudate nucleus in glioma patients having undergone magnetic resonance imaging (MRI) before and after RT.

Materials and methods: Subcortical volumes were measured using T1-weighted MRI from patients before RT (N = 91) and from longitudinal follow-ups acquired in three-monthly intervals (N = 349). The volumes were normalized to the baseline values, while excluding structures touching the clinical target volume (CTV) or abnormal tissue seen on FLAIR imaging. A multivariate linear effects model was used to determine if time after RT and mean RT dose delivered to the corresponding structures were significant predictors of tissue atrophy.

Results: The hippocampus, amygdala, thalamus, putamen, and pallidum showed significant atrophy after RT as function of both time after RT and mean RT dose delivered to the corresponding structure. Only the caudate showed no dose or time dependant atrophy. Conversely, the hippocampus was the structure with the highest atrophy rate of 5.2 % after one year and assuming a mean dose of 30 Gy.

Conclusion: The hippocampus showed the highest atrophy rates followed by the thalamus and the amygdala. The subcortical structures here found to decrease in volume indicative of radiosensitivity should be the focus of future studies investigating the relationship between neurocognitive decline and RT.

Abbreviations: CSF, cerebrospinal fluid; CT, computed tomography; CTV, clinical target volume; GM, grey matter; GTV, gross tumour volume; MNI, Montreal Neurological Institute; MRI, magnetic resonance imaging; PTV, planning target volume; ROI, region of interest; RT, radiotherapy; T1w, T1-weighted; TBV, tumour bed volume; WM, white matter.

* Corresponding author at: Department of Radiotherapy and Radiation Oncology, Faculty of Medicine and University Hospital Carl Gustav Carus of Technische Universität Dresden, Fetscherstrasse 74, 01307 Dresden, Germany.
E-mail address: esther.troost@uniklinikum-dresden.de (E.G.C. Troost).

https://doi.org/10.1016/j.ctro.2022.07.003
Received 22 June 2022; Accepted 7 July 2022
Available online 20 July 2022

Introduction

Radiotherapy (RT), possibly combined with chemotherapy, is a standard treatment option after surgery for primary brain tumour patients. However, RT may cause cognitive dysfunction and can impact the patients' quality of life, particularly in long-term survivors [1–3]. RT has also been shown to cause a number of structural and functional changes to surrounding normal appearing brain tissue as seen on magnetic resonance imaging (MRI) [4]. Brain tissue atrophy is one of these observed changes and has been directly correlated to the delivered radiation dose [5,6].

The hippocampus has been in the focus when investigating RT-related side-effects since it plays a key role in cognitive decline during normal ageing and neurodegenerative diseases [7]. Previous studies have found correlations between radiation dose to the hippocampus, hippocampal atrophy, and neurocognitive decline [8–10]. This has recently led to studies investigating the use of hippocampal avoidance in RT to preserve cognitive function [11,12]. Moreover, early evidence suggests causal correlation between RT-induced hippocampal atrophy and cognitive decline [13]. Thus, hippocampal atrophy measures may have the potential to become objective markers of RT damage and subsequently of neurocognitive decline.

Other subcortical structures, which also play a major role in cognition include the thalamus, amygdala and the basal ganglia [14,15]. However, to date only few studies evaluated atrophy rates of subcortical regions in the same patient cohort in comparison to the radiation dose and/or interval after RT, in order to determine the structures' respective radiosensitivities [16,17].

In the era of highly conformal RT using photons and particles, recommendations harmonizing the delineation of the substructures as well as of prescribing radiation dose have been published [18]. These strive to determine objective outcome parameters possibly supporting the use of particle therapy. To complement the previous studies and consolidate the results, a longitudinal study involving periodic MR monitoring over the course of three years was established [16,17]. The goal of this study was to compare volumes of the hippocampus, amygdala, thalamus, putamen, pallidum and caudate nucleus on magnetic resonance imaging (MRI) in the same patient cohort before and after radio(chemo)therapy, to determine whether these structures exhibit radiation-induced atrophy depending on the combined influence of RT dose and time, and whether atrophy rates differ between structures.

Methods

Patient cohorts

Patient cohorts and exclusion criteria were identical to our previous study on cerebellar atrophy after radio(chemo)therapy [5]. In summary, data from two different prospective studies was combined for this analysis. Study A (NCT02824731) comprised longitudinal data of grade I-IV glioma patients (ethics approval EK22012016). Study B (NCT01873469) included grade IV glioblastoma patients as part of a prospective, longitudinal study investigating the effect of 11C-methionine positron emission tomography (PET)/MR for tailoring the treatment of patients with glioblastoma [19], approved by the local ethics committee (EK41022013, BO-EK-167052020). Comparable study design and contouring suggest the same dosage distribution in normal tissue, thus allowing the combination of the two studies. Table 1 contains the patient characteristics of both studies.

Gross tumour resection was performed in most patients prior to radio(chemo)therapy. Baseline MR images were acquired after surgery and typically two weeks before the start of radio(chemo)therapy. Follow-up MRIs were first acquired approximately three months after the end of radiotherapy and at three-monthly intervals thereafter. However, patients occasionally skipped some of the follow-up MRs or received clinical follow-up MRs at other centres, which were not used for analysis in this study. The scans were generally performed until either patient status worsened or patients required further clinical intervention due to clinical progression. Patients with a baseline MRI and at least one follow-up MRI were included in this analysis. Patients who underwent re-irradiation, had severe motion artefacts on MRI, aspergillus infection (one patient) or an external head trauma (one patient) were excluded from the analysis.

Data acquisition

All MRI data were acquired on a 3 Tesla Philips Ingenuity PET/MR scanner (Philips, Eindhoven, The Netherlands) using an eight channel head coil.

T1-weighted (T1w) MR images were used for the segmentation of subcortical structures. In study A, T1w images were acquired using a 3D gradient spoiled echo sequence acquired in sagittal orientation with 1 mm isotropic resolution. In study B, T1w images were acquired using a 3D Turbo Field Echo sequence acquired in sagittal orientation at 1 mm isotropic resolution.

Conventional FLAIR images were used for each patient and timepoint to identify abnormal tissue and create abnormal tissue regions of interest (ROIs).

Radiation treatment planning

Computed tomography (CT) scans for radiation treatment planning were performed prior to radio(chemo)therapy with the patient positioned supine with an individual head support and mask. For radiation treatment planning, the CTs were co-registered with the post-surgery MRI scans (T1w, T2-weighted, T1w with contrast agent) to define the tumour bed and potential residual tumour (tumour bed volume; TBV, or gross tumour volume; GTV, respectively). For the patients of study A, the TBV (including the GTV) was expanded by a 1.5–2 cm isotropic margin for grade III and IV tumours, respectively and corrected for anatomical boundaries, to derive the clinical target volume (CTV). The prescribed total dose to the CTV was typically either 54 Gy(RBE) or 60 Gy(RBE) depending on tumour histology and delivered in 2 Gy(RBE)-fractions. Radiotherapy using protons with a maximal beam energy of 230 MeV was either performed by the double scattering technique planned on XiO (Version V5.00.02, Elekta AB, Stockholm, Sweden) with field shaping using lateral apertures and range compensators, or with pencil beam scanning planned on RayStation (Version 6.0, RaySearch, Stockholm, Sweden) using single-field uniform dose optimization. For photon beam

Table 1
Patient demographics. TMZ – temozolomide, PCV – procarbazine, lomustine (CCNU) and vincristine, Ph – photon therapy, H+ – proton therapy.

	study A	study B	study A + B
Number of patients [n]			
total/male/female	24/11/13	67/38/29	91/49/42
Age at baseline [years]			
mean ± std	45.6 ± 14.5	54.7 ± 13.9	52.3 ± 14.5
range [min – max]	[20.1 – 76.7]	[23.2 – 81.8]	[20.1 – 81.8]
Glioma grade [n]			
grade I/II/III/IV	1/3/13/7	0/0/0/67	1/3/13/74
RTx treatment [n]			
Ph/H+/mix	4/19/1	48/19/0	52/38/1
Chemotherapy [n]			
TMZ/PCV/none	7/5/12	67/0/0	74/5/12
Follow-ups			
mean number of follow-ups [n]	4.4 ± 3.0	3.6 ± 3.2	3.8 ± 3.2
mean follow-up period [days]	444.8 ± 311.4	422.2 ± 438.5	428.1 ± 407.3
range follow-up period [days]	[85 – 1073]	[63 – 1874]	[63 – 1874]

irradiation a planning target volume (PTV) was created by increasing the CTV using an isotropic margin of 0.5 cm. Detailed information about the treatment planning system for photon beam irradiation, and dose calculation of study B is provided by Seidlitz *et al.* [19]. Proton and photon therapy effect on tumour control were expected to be equal, since the generation of the CTV was similar for proton and photon treatment and the proton dose was normalized to a factor of 1.1 for relative biological effectiveness. The constraint dose to the organs at risk was determined according to recent guidelines regarding normal tissue complication probability based in the ICRU recommendations [20–23]. For this analysis, the planning CTs and corresponding dose maps were retrieved from the planning workstation.

Data processing

Binary labels for the hippocampus, amygdala, thalamus, putamen, pallidum, and caudate nucleus were generated for each T1w image by non-linear warping the Montreal Neurological Institute (MNI) 152 brain atlas [24] and corresponding Harvard-Oxford subcortical atlas provided by the "FMRIB Software Library" (FSL) [25] to each T1w image using "Advanced Normalization Tools" (ANTs) [26,27]. Left and right structures were considered separately. For the caudate nucleus, atlas labels for "caudate" and "accumbens" were merged because both structures are difficult to distinguish reliably on standard T1w imaging.

Each T1w image was segmented into grey matter (GM), white matter (WM) and cerebrospinal fluid (CSF) using SPM12 (Statistical Parametric Mapping: https://www.fil.ion.ucl.ac.uk/spm/) after censoring abnormal tissue using abnormal tissue ROIs created from the corresponding FLAIR images at that particular timepoint [28]. The sum of all GM and WM probabilities within each subcortical label was used to calculate the corresponding subcortical volume. Subcortical structures were excluded from the analysis if any part was within the CTV. Subcortical volumes were also excluded at individual timepoints if any part was within the abnormal tissue ROI at that time. Fig. 1 illustrates the subcortical segmentation process for a grade III glioma patient.

The mean dose delivered to each subcortical structure was calculated by rigidly co-registering the planning CT and corresponding dose maps to the baseline T1w images.

Statistical analysis

Relative subcortical volumes V_{rel} were calculated for each patient as ratios to their corresponding pre-radiotherapy baseline values.

Analysis was carried out in R using separate multivariate linear mixed effects models for each left and right subcortical volume [29]. Structures were evaluated separately for the left and right hemisphere to guarantee the coverage of the full irradiation dose range in the each dataset (compare supplementary Table S1). Relative subcortical volumes were used as the response variables and the patient ID as grouping variable. Multiple univariate analyses with time after radiotherapy, mean radiation dose, patient age, gender, low grade (grade I-II) or high grade (grade III-IV) tumour, radiotherapy modality (proton/photon), chemotherapy (yes/no) were first performed to determine which effects to consider in the subsequent multivariate linear mixed effects models. We also compared the subcortical atrophy rates to those of the cerebellum as published previously [5].

Results

In total, 91 patients with baseline MRIs and 349 follow-up MRIs were eligible for this study (see Table 1). The actual number of structures in the models varied, since structures were excluded if any part was within either the CTV or the abnormal ROI. An overview of the number of structures and corresponding follow-ups and mean RT doses is given in supplementary Table S1.

The general trend that subcortical structures lost volume over time is illustrated in supplementary Figure S1. Trendlines of the relative subcortical volumes are colour-coded according to the mean dose

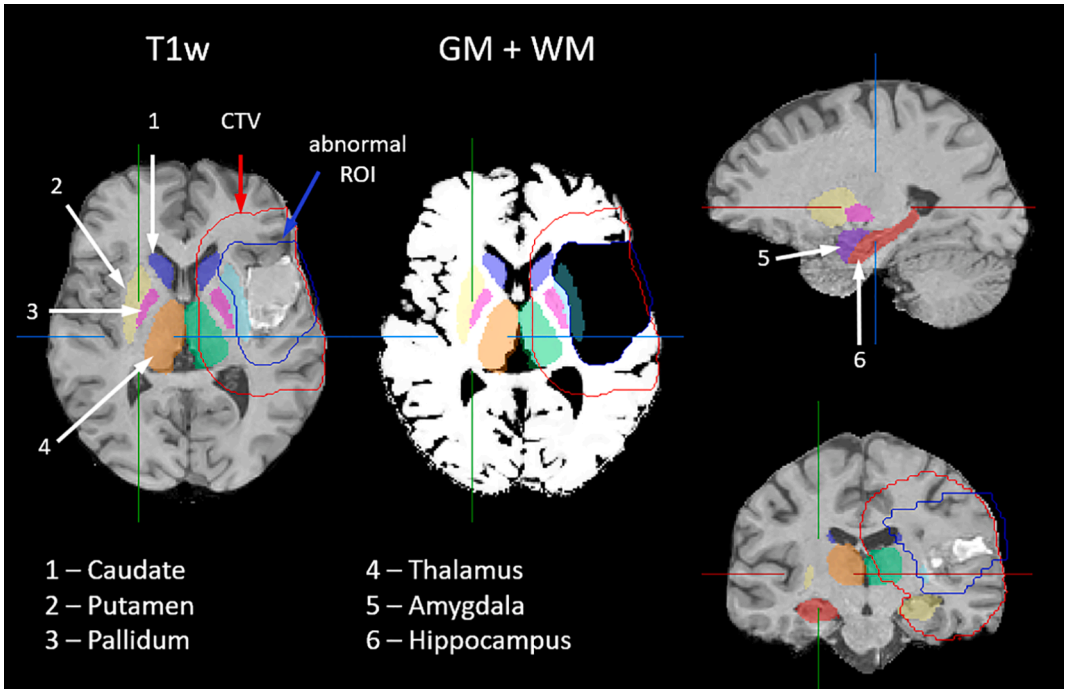

Fig. 1. Segmentation of the subcortical structures shown on the baseline T1w image for a patient after resection of a grade III glioma. Subcortical labels are transferred from MNI152 brain atlas to each T1w image by non-linear coregistration. T1w images were segmented into GM, WM and CSF and the sum of GM + WM probabilities within each subcortical label was used to calculate the corresponding subcortical volume. Structures with any parts touching the CTV (red contour) or abnormal ROI (blue contour) were excluded from the analysis. (For interpretation of the references to colour in this figure legend, the reader is referred to the web version of this article.)

delivered to the corresponding structure for all patients.

Univariate analysis for the twelve structures revealed that the mean dose and time after RT were the most common significant predictors of the subcortical volumes, whereas patient age, gender, low grade (grade I-II) or high grade (grade III-IV) tumour, radiotherapy modality (proton/photon), and chemotherapy (yes/no) were no significant predictors (see supplementary Table S2). Consequently, for the final analysis we used the following multivariate linear mixed effects model:

$$V_{\mathrm{rel}} = a \times dose + b \times time + c \times time \times dose + d \quad (1)$$

The model coefficients are given in Table 2. Significant volume loss occurred in all structures except the caudate nucleus. Atrophy increased with higher mean radiation dose and with increasing time after radiotherapy. Visual representations of these regression results are plotted in Fig. 2 considering a time of 1, 2 and 3 years after radiotherapy and a varying mean dose between 0 and 60 Gy delivered to the corresponding structures. This reveals that the hippocampus had the highest atrophy rates, followed by the thalamus and amygdala. The caudate nucleus on the other hand, showed no significant volume changes. For the cerebellum, we previously found age to be an additional significant predictor of atrophy besides dose and time [5]. To allow for direct comparison of the atrophy rates, the multivariate model in [Eq. (1)] was also applied to the cerebellum data and corresponding values are given in Table 2 and Fig. 2.

Discussion

In this study, we compared volumes of six subcortical structures before and after radio(chemo)therapy in the same cohort of proton and photon irradiated patients over a MR monitoring time of three years

Table 2
Results of the multivariate linear mixed effects models $V_{\mathrm{rel}} = a \times dose + b \times time + c \times time \times dose + d$ for all structures.

	Right				Left			
	Hippocampus							
	value	sd error	t-value	p-value	value	sd error	t-value	p-value
Intercept	9.92E−01	4.86E−03	204.17	<0.001	9.87E−01	5.40E−03	182.85	<0.001
Dose	−2.58E−04	1.91E−04	−1.36	0.181	−4.03E−04	2.02E−04	−1.99	0.050
Time	−1.12E−05	5.15E−06	−2.18	0.031	−1.21E−05	7.72E−06	−1.57	0.117
Time × dose	−2.80E−06	3.44E−07	−8.05	<0.001	−2.20E−06	3.72E−07	−5.84	<0.001
	Amygdala							
Intercept	9.96E−01	6.45E−03	154.38	<0.001	1.00E+00	8.70E−03	115.07	<0.001
Dose	−3.31E−04	2.09E−04	−1.58	0.119	−3.67E−04	2.95E−04	−1.24	0.219
Time	−4.30E−06	7.84E−06	−0.55	0.582	−1.09E−05	8.29E−06	−1.32	0.189
Time × dose	−1.90E−06	4.29E−07	−4.39	<0.001	−1.20E−06	3.61E−07	−3.43	0.001
	Putamen							
Intercept	1.01E+00	5.83E−03	172.62	<0.001	1.00E+00	3.97E−03	252.04	<0.001
Dose	−3.84E−04	1.63E−04	−2.35	0.022	−5.83E−05	1.21E−04	−0.48	0.631
Time	−6.00E−06	8.07E−06	−0.75	0.457	−2.10E−05	5.98E−06	−3.51	0.001
Time × dose	−1.10E−06	2.70E−07	−4.19	<0.001	−5.00E−07	1.82E−07	−2.81	0.005
	Thalamus							
Intercept	9.95E−01	8.23E−03	120.99	<0.001	9.96E−01	5.40E−03	184.42	<0.001
Dose	−3.01E−04	2.10E−04	−1.43	0.158	−3.20E−04	1.53E−04	−2.09	0.041
Time	7.60E−06	1.21E−05	0.63	0.531	6.80E−06	8.00E−06	0.85	0.398
Time × dose	−2.20E−06	3.69E−07	−5.95	<0.001	−2.00E−06	2.73E−07	−7.18	<0.001
	Pallidum							
Intercept	1.01E+00	8.00E−03	125.80	<0.001	1.01E+00	6.44E−03	156.20	<0.001
Dose	−2.98E−04	1.96E−04	−1.52	0.133	−2.59E−04	1.76E−04	−1.47	0.146
Time	−3.70E−06	1.03E−05	−0.36	0.718	2.30E−06	8.67E−06	0.26	0.792
Time × dose	−1.30E−06	3.09E−07	−4.14	<0.001	−1.60E−06	2.45E−07	−6.53	<0.001
	Caudate							
Intercept	9.98E−01	6.31E−03	158.22	<0.001	9.93E−01	4.90E−03	202.81	<0.001
Dose	−1.31E−04	1.69E−04	−0.77	0.442	1.34E−04	1.41E−04	0.95	0.344
Time	−2.33E−05	1.33E−05	−1.76	0.081	−1.72E−05	9.41E−06	−1.83	0.069
Time × dose	0.00E+00	3.76E−07	0.07	0.946	0.00E+00	3.36E−07	0.00	1.000

	Cerebellum			
Intercept	1.00E+00	1.27E−03	787.56	<0.001
Dose	−5.84E−04	2.26E−04	−2.59	0.011
Time	−8.80E−06	1.61E−06	−5.45	<0.001
Time × dose	−3.40E−06	4.25E−07	−8.03	<0.001

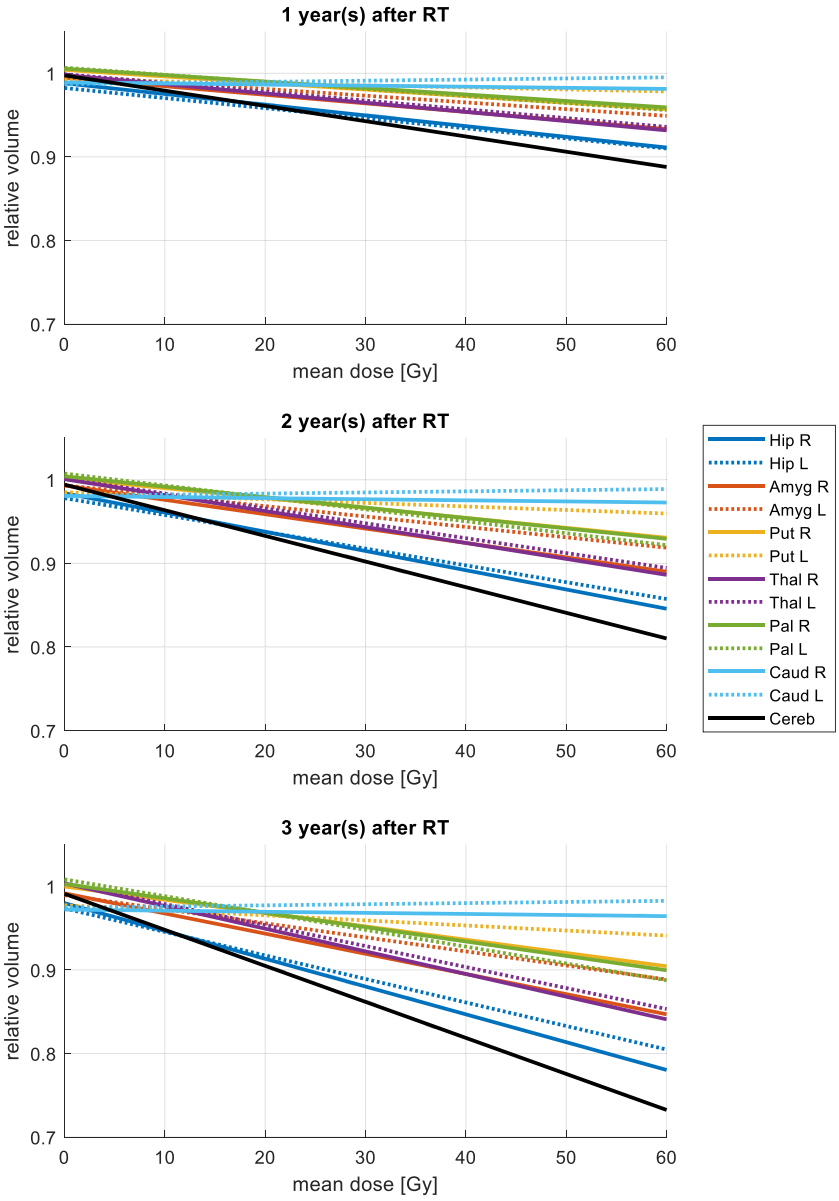

Fig. 2. Predicted relative volumes 1, 2 and 3 years after RT, respectively according to the multivariate models given in Table 2.

after RT and found the highest atrophy rate in the hippocampus followed by the thalamus and amygdala. Mean dose delivered to the corresponding structures and time after radiotherapy were significant predictors of volume loss.

Two previous studies compared volumes of the same subcortical structures before and after radiotherapy. Takeshita et al. [16] analysed 20 patients with brain metastases receiving whole brain RT of 30 Gy and found the hippocampus to be the only structure showing significant time-dependent atrophy with an average volume reduction of 9.2 % eight to eleven months after whole brain RT. In a study of 31 grade II-IV glioma patients, Nagtegaal et al. [17] found atrophy correlating significantly with the radiation dose in all subcortical structures except the caudate nucleus one year after RT. As an extension of the above mentioned studies considering the influence of time and irradiation dose separately, our study provided a combined assessment on the influence of radiation dose and time from RT on volume changes. The longitudinal observation period allowed for investigation of long term effects of irradiation, while the inclusion of the proton treated patients provided the opportunity to examine changes at low irradiation dose. Other studies looked at the hippocampus and amygdala separately. Huynh-Le et al. [30] and Seibert et al. [31] assessed the same cohort of 52 primary brain tumour patients one year after RT and found significant dose dependent atrophy of the amygdala and hippocampus, respectively. Prust et al. [32] found no significant volume reduction of the hippocampus in 14 glioblastoma patients in a longitudinal observation up to 35 weeks after RT. For these studies, the predicted volume reductions six to twelve months after RT and assuming a mean dose of 30 Gy are compared to the results of this study in Table 3. In summary, significant dose dependant atrophy was found in three out of four studies for the amygdala and in five out of six studies for the hippocampus. Predicted volume reductions were very similar in all cases. Interestingly, the caudate was the only structure, consistently showed no significant reduction in volume after RT. The reason for this is unclear and warrants further investigation in future studies. Results for the pallidum, putamen, thalamus are more ambivalent. While Takeshita et al. [16] reported no significant volume reductions, Nagtegaal et al. [17] found the highest volume reductions in these structures one year after RT. However, the atrophy rates were an order of magnitude higher compared to all other results (see Table 3).

Atrophy rates of the subcortical volumes were comparable to those

Table 3
Comparison of predicted volume reductions six to twelve months after RT found in literature, assuming a mean dose of 30 Gy. RT – radiotherapy, WBRT – whole brain radiotherapy.

Publication	cohort	number of patients	time after RT [months]	Hippocampus	Amygdala	Putamen	Thalamus	Pallidum	Caudate
[17]	RT of grade II-IV gliomas	31	12	**4.9 %**	**9.0 %**	**24.3 %**	**34.5 %**	**41.2 %**	3.0 %
[16]	WBRT of METs with 30 Gy	20	6–10	**5.7 %**	4.9 %	2.5 %	6.9 %	−2.4 %	9.7 %
			8–11	**9.2 %**	-	-	-	-	-
[30]	RT of primary brain tumours	52	12	-	**5.1 %**	-	-	-	-
[31]	identical to [30]			**6 %***	-	-	-	-	-
[32]	RT of glioblastoma patients	14	<6	n.s.	-	-	-	-	-
This study	RT of grade II-IV gliomas	91	12	**5.2 %****	**3.1 %****	**1.7 %****	**3.4 %****	**1.8 %****	1.2 %**

** mean of left and right structure.
* mean dose > 40 Gy.
– not assessed.
bold significant.
n.s. no significant change.

found previously by our group in the cerebellum [5]. Although the cerebellum shows the highest atrophy rates at a given mean dose (Fig. 2), the highest observed mean dose in the cerebellum was 17 Gy [5] which is much lower than the mean doses up to 58 Gy that can be seen in the much smaller subcortical structures (see supplementary Table S1), considering conformal RT of cerebral tumours.

RT induced volume loss of the hippocampus has previously been linked to cognitive decline [13] and recent studies have investigated the impact of hippocampal dose sparing on patient cognition. On the one hand, in a phase III trial with 518 brain metastases patients treated with 30 Gy whole brain RT, Brown et al. [12] showed that hippocampal avoidance better preserved cognitive function, specifically executive function, learning and memory. On the other hand, in another phase III trial with 168 small cell lung cancer patients by Belderbos et al. [11] no significant difference in cognitive decline between the hippocampal avoidance group and conventionally treated group was found.

Our study is characterized by the longitudinal analysis of multiple GM structures based on a large patient data set and combined assessment of the effects of dose and time on volume changes, providing a validation and extension of previously published results. To the best of our knowledge, this is the first study to include proton irradiated patients, which enabled to obtain information on tissue changes in areas of low dose impact. The results of the linear regression model will provide a comparison for future studies and can be used in clinical applications for decisions on the type of irradiation or sparing of specific structures.

Limitations of this study are the lack of neurocognitive function tests, which have not been acquired in this assessment. However, prospective studies are currently ongoing. Additionally, because of patient dropout over time, the number of available MRIs reduced continuously over time. Nevertheless, we were able to acquire sufficient data points for volume measurements beyond one year after RT (see supplementary Table S1). Although guidelines exist for contouring brain substructures for RT planning [18], here we used an automated segmentation method to allow for a consistent retrospective inter- and intra-patient volume measurement.

Future work is needed to determine which amount of hippocampal atrophy leads to clinically relevant levels of cognitive decline and thus develop corresponding normal tissue complication probability models [33]. High resolution MR imaging of the hippocampus could also be used to determine more precisely what anatomical changes are occurring in the hippocampus after RT [34]. Connections between cognitive decline and atrophy after RT of the other subcortical structures such as the amygdala and thalamus also need to be explored.

Declaration of Competing Interest

The authors declare the following financial interests/personal relationships which may be considered as potential competing interests: In the past 5 years, Dr. Michael Baumann attended an advisory board meeting of MERCK KGaA (Darmstadt), for which the University of Dresden received a travel grant. He further received funding for his research projects and for educational grants to the University of Dresden by Teutopharma GmbH (2011–2015), IBA (2016), Bayer AG (2016–2018), Merck KGaA (2014-open), Medipan GmbH (2014–2018). He is on the supervisory board of HI-STEM gGmbH (Heidelberg) for the German Cancer Research Center (DKFZ, Heidelberg) and also member of the supervisory body of the Charité University Hospital, Berlin. As former chair of OncoRay (Dresden) and present CEO and Scientific Chair of the German Cancer Research Center (DKFZ, Heidelberg), he has been or is still responsible for collaborations with a multitude of companies and institutions, worldwide. In this capacity, he discussed potential projects with and has signed/signs contracts for his institute(s) and for the staff for research funding and/or collaborations with industry and academia, worldwide, including but not limited to pharmaceutical corporations like Bayer, Boehringer Ingelheim, Bosch, Roche and other corporations like Siemens, IBA, Varian, Elekta, Bruker and others. In this role, he was/is further responsible for commercial technology transfer activities of his institute(s), including the DKFZ-PSMA617 related patent portfolio [WO2015055318 (A1), ANTIGEN (PSMA)] and similar IP portfolios.

Within the past years, Dr. Krause received funding for her research projects by IBA (2016), Merck KGaA (2014–2018 for preclinical study; 2018–2020 for clinical study), Medipan GmbH (2014–2018), Attomol GmbH (2019–2021), GA Generic Assays GmbH (2019–2021), BTU Cottbus-Senftenberg (2019–2021), Gesellschaft für medizinische und wissenschaftliche genetische Analysen (2019–2021), Lipotype GmbH (2019–2021), PolyAn GmbH (2019–2021).

Dr. Troost received funding for her research projects by Attomol GmbH (2019–2021), GA Generic Assays GmbH (2019–2021), BTU Cottbus-Senftenberg (2019–2021), Gesellschaft für medizinische und wissenschaftliche genetische Analysen (2019–2021), Lipotype GmbH (2019–2021), PolyAn GmbH (2019–2021).

Dr. Baumann, Dr. Krause and Dr. Troost confirm that to the best of his knowledge none of the above funding sources were involved in the preparation of this paper.

The other authors have nothing to disclose.

Acknowledgements

We thank all patients who participated in the respective studies. We also want to thank the clinical trials centre, especially the study nurses Annett Petzold, Susanne Klöber, Luisa Schünzel and Aline Lähner. This work was partly funded by the National Center for Tumor Diseases (NCT), Partner Site Dresden; Deutscher Akademischer Austauschdienst (DAAD, personal grant FR); and the German Cancer Consortium, Partner Site Dresden.

Appendix A. Supplementary data

Supplementary data to this article can be found online at https://doi.org/10.1016/j.ctro.2022.07.003.

References

[1] Cayuela N, Jaramillo-Jiménez E, Càmara E, Majós C, Vidal N, Lucas A, et al. Cognitive and brain structural changes in long-term oligodendroglial tumor survivors. Neuro-Oncology 2019;21(11):1470–9. https://doi.org/10.1093/neuonc/noz130.

[2] Douw L, Klein M, Fagel SS, van den Heuvel J, Taphoorn MJB, Aaronson NK, et al. Cognitive and radiological effects of radiotherapy in patients with low-grade glioma: long-term follow-up. The Lancet Neurology 2009;8(9):810–8. https://doi.org/10.1016/S1474-4422(09)70204-2.

[3] Surma-aho O, Niemela M, Vilkki J, Kouri M, Brander A, Salonen O, et al. Adverse long-term effects of brain radiotherapy in adult low-grade glioma patients. Neurology 2001;56(10):1285–90. https://doi.org/10.1212/WNL.56.10.1285.

[4] Witzmann K, Raschke F, Troost EGC. MR image changes of normal-appearing brain tissue after radiotherapy. Cancers 2021;13(7):1573. https://doi.org/10.3390/cancers13071573.

[5] Raschke F, Seidlitz A, Wesemann T, Löck S, Jentsch C, Platzek I, et al. Dose dependent cerebellar atrophy in glioma patients after radio(chemo)therapy. Radiother Oncol 2020;150:262–7. https://doi.org/10.1016/j.radonc.2020.07.044.

[6] Petr J, Platzek I, Hofheinz F, Mutsaerts HJMM, Asllani I, van Osch MJP, et al. Photon vs. proton radiochemotherapy: Effects on brain tissue volume and perfusion. Radiother Oncol 2018;128(1):121–7. https://doi.org/10.1016/j.radonc.2017.11.033.

[7] Tobin MK, Musaraca K, Disouky A, Shetti A, Bheri A, Honer WG, et al. Human hippocampal neurogenesis persists in aged adults and Alzheimer's disease patients. Cell Stem Cell 2019;24(6):974–982.e3. https://doi.org/10.1016/j.stem.2019.05.003.

[8] Ma TM, Grimm J, McIntyre R, Anderson-Keightly H, Kleinberg LR, Hales RK, et al. A prospective evaluation of hippocampal radiation dose volume effects and memory deficits following cranial irradiation. Radiother Oncol 2017;125(2):234–40. https://doi.org/10.1016/j.radonc.2017.09.035.

[9] Gondi V, Hermann BP, Mehta MP, Tomé WA. Hippocampal dosimetry predicts neurocognitive function impairment after fractionated stereotactic radiotherapy for benign or low-grade adult brain tumors. Internat J Radiat Oncol Biol Phys 2012;83(4):e487–93. https://doi.org/10.1016/j.ijrobp.2011.10.021.

[10] Hernández-Rabaza V, Llorens-Martín M, Velázquez-Sánchez C, Ferragud A, Arcusa A, Gumus HG, et al. Inhibition of adult hippocampal neurogenesis disrupts contextual learning but spares spatial working memory, long-term conditional rule retention and spatial reversal. Neuroscience 2009;159(1):59–68. https://doi.org/10.1016/j.neuroscience.2008.11.054.

[11] Belderbos JSA, De Ruysscher DKM, De Jaeger K, Koppe F, Lambrecht MLF, Lievens YN, et al. Phase 3 randomized trial of prophylactic cranial irradiation with or without hippocampus avoidance in SCLC (NCT01780675). J Thoracic Oncol 2021;16(5):840–9. https://doi.org/10.1016/j.jtho.2020.12.024.

[12] Brown PD, Gondi V, Pugh S, Tome WA, Wefel JS, Armstrong TS, et al. Hippocampal avoidance during whole-brain radiotherapy plus memantine for patients with brain metastases: Phase III trial NRG oncology CC001. JCO 2020;38(10):1019–29. https://doi.org/10.1200/JCO.19.02767.

[13] Lv X, He H, Yang Y, Han L, Guo Z, Chen H, et al. Radiation-induced hippocampal atrophy in patients with nasopharyngeal carcinoma early after radiotherapy: a longitudinal MR-based hippocampal subfield analysis. Brain Imaging Behav 2019;13(4):1160–71. https://doi.org/10.1007/s11682-018-9931-z.

[14] Catani M, Dell'Acqua F, Thiebaut de Schotten M. A revised limbic system model for memory, emotion and behaviour. Neurosci Biobehav Rev 2013;37(8):1724–37. https://doi.org/10.1016/j.neubiorev.2013.07.001.

[15] Herrero M-T, Barcia C, Navarro J. Functional anatomy of thalamus and basal ganglia. Child's Nervous System 2002;18(8):386–404. https://doi.org/10.1007/s00381-002-0604-1.

[16] Takeshita Y, Watanabe K, Kakeda S, Hamamura T, Sugimoto K, Masaki H, et al. Early volume reduction of the hippocampus after whole-brain radiation therapy: an automated brain structure segmentation study. Jpn J Radiol 2020;38(2):118–25. https://doi.org/10.1007/s11604-019-00895-3.

[17] Nagtegaal SH, David S, Philippens ME, Snijders TJ, Leemans A, Verhoeff JJ. Dose-dependent volume loss in subcortical deep grey matter structures after cranial radiotherapy. Clin Transl Radiat Oncol 2021;26:35–41. https://doi.org/10.1016/j.ctro.2020.11.005.

[18] Eekers DBP, in 't Ven L, Roelofs E, Postma A, Alapetite C, Burnet NG, et al. The EPTN consensus-based atlas for CT- and MR-based contouring in neuro-oncology. Radiother Oncol 2018;128(1):37–43. https://doi.org/10.1016/j.radonc.2017.12.013.

[19] Seidlitz A, Beuthien-Baumann B, Löck S, Jentsch C, Platzek I, Zöphel K, et al. Final results of the prospective biomarker trial PETra: [11C]-MET-accumulation in postoperative PET/MRI predicts outcome after radiochemotherapy in glioblastoma. Clin Cancer Res 2021;27(5):1351–60. https://doi.org/10.1158/1078-0432.CCR-20-1775.

[20] Mayo C, Yorke E, Merchant TE. Radiation associated brainstem injury. Int J Radiat Oncol Biol Phys 2010;76(3 Suppl):S36–41. https://doi.org/10.1016/j.ijrobp.2009.08.078.

[21] Mayo C, Martel MK, Marks LB, Flickinger J, Nam J, Kirkpatrick J. Radiation dose-volume effects of optic nerves and chiasm. Int J Radiat Oncol Biol Phys 2010;76(3 Suppl):S28–35. https://doi.org/10.1016/j.ijrobp.2009.07.1753.

[22] Lawrence YR, Li XA, el Naqa I, Hahn CA, Marks LB, Merchant TE, et al. Radiation dose-volume effects in the brain. Int J Radiat Oncol Biol Phys 2010;76(3 Suppl):S20–7. https://doi.org/10.1016/j.ijrobp.2009.02.091.

[23] Lambrecht M, Eekers DBP, Alapetite C, Burnet NG, Calugaru V, Coremans IEM, et al. Radiation dose constraints for organs at risk in neuro-oncology; the European Particle Therapy Network consensus. Radiother Oncol 2018;128(1):26–36. https://doi.org/10.1016/j.radonc.2018.05.001.

[24] Grabner G, Janke AL, Budge MM, Smith D, Pruessner J, Collins DL. Symmetric atlasing and model based segmentation: an application to the hippocampus in older adults. In: Hutchison D, Kanade T, Kittler J, Kleinberg JM, Mattern F, Mitchell JC, editors. medical image computing and computer-assisted intervention – MICCAI 2006. Springer, Berlin Heidelberg: Berlin, Heidelberg; 2006. p. 58–66.

[25] Jenkinson M, Beckmann CF, Behrens TEJ, Woolrich MW, Smith SM. FSL. NeuroImage 2012;62(2):782–90. https://doi.org/10.1016/j.neuroimage.2011.09.015.

[26] Avants BB, Tustison NJ, Song G, Cook PA, Klein A, Gee JC. A reproducible evaluation of ANTs similarity metric performance in brain image registration. NeuroImage 2011;54(3):2033–44. https://doi.org/10.1016/j.neuroimage.2010.09.025.

[27] Tustison NJ, Avants BB. Explicit B-spline regularization in diffeomorphic image registration. Front Neuroinform 2013;7. https://doi.org/10.3389/fninf.2013.00039.

[28] Gommlich A, Raschke F, Petr J, Seidlitz A, Jentsch C, Platzek I, et al. Overestimation of grey matter atrophy in glioblastoma patients following radio (chemo)therapy. Magn Reson Mater Phy 2022;35(1):145–52. https://doi.org/10.1007/s10334-021-00922-3.

[29] R.C. Team. R: A Language and Environment for Statistical Computing. R Foundation for Statistical Computing. Vienna, Austria; 2019; Available from: https://www.R-project.org/.

[30] Huynh-Le M-P, Karunamuni R, Moiseenko V, Farid N, McDonald CR, Hattangadi-Gluth JA, et al. Dose-dependent atrophy of the amygdala after radiotherapy. Radiother Oncol 2019;136:44–9. https://doi.org/10.1016/j.radonc.2019.03.024.

[31] Seibert TM, Karunamuni R, Bartsch H, Kaifi S, Krishnan AP, Dalia Y, et al. Radiation dose-dependent hippocampal atrophy detected with longitudinal volumetric magnetic resonance imaging. Internat J Radiat Oncol Biol Phys 2017;97(2):263–9. https://doi.org/10.1016/j.ijrobp.2016.10.035.

[32] Prust MJ, Jafari-Khouzani K, Kalpathy-Cramer J, Polaskova P, Batchelor TT, Gerstner ER, et al. Standard chemoradiation for glioblastoma results in progressive brain volume loss. Neurology 2015;85(8):683–91. https://doi.org/10.1212/WNL.0000000000001861.

[33] Dutz A, Lühr A, Agolli L, Troost EGC, Krause M, Baumann M, et al. Development and validation of NTCP models for acute side-effects resulting from proton beam therapy of brain tumours. Radiother Oncol 2019;130:164–71. https://doi.org/10.1016/j.radonc.2018.06.036.

[34] Donix M, Burggren AC, Scharf M, Marschner K, Suthana NA, Siddarth P, et al. APOE associated hemispheric asymmetry of entorhinal cortical thickness in aging and Alzheimer's disease. Psych Res Neuroimag 2013;214(3):212–20. https://doi.org/10.1016/j.pscychresns.2013.09.006.